JOURNAL OF Applied Polymer SCIENCE

Application of the dry-spinning method to produce poly(ε-caprolactone) fibers containing bovine serum albumin laden gelatin nanoparticles

Bahareh Azimi,[1,2] Parviz Nourpanah,[1] Mohammad Rabiee,[3] Shahram Arbab,[4] Maria Grazia Cascone,[2] Andrea Baldassare,[2] Luigi Lazzeri[2]

[1]Department of Textile Engineering, Amirkabir University of Technology, 424 Hafez Ave, Tehran, 15875-4413, Iran
[2]Department of Civil and Industrial Engineering, University of Pisa, largo Lucio Lazzarino 1 56122, Pisa, Italy
[3]Department of Biomedical Engineering, Amirkabir University of Technology, Tehran, Iran
[4]Department of Textile Engineering, ATMT Research Institute, Amirkabir University of Technology, Tehran, Iran
Correspondence to: B. Azimi (E-mail: azimi89@aut.ac.ir)

ABSTRACT: We designed and manufactured a polymeric system with combined hydrophilic–hydrophobic properties by loading gelatin nanoparticles (GNPs) containing bovine serum albumin (BSA) into poly(ε-caprolactone) (PCL) fibers. Our ultimate goal was to create a device capable of carrying and releasing protein drugs. Such a system could find several biomedical applications, such as those in controlled release systems, surgical sutures, and bioactive scaffolds for tissue engineering. A two-step desolvation method was used to produce GNPs, whereas PCL fibers were produced by a dry-spinning method. The morphological, mechanical, and thermal properties of the produced system were investigated, and the distribution of nanoparticles both inside and on the surface of the fibers was examined. The effect of the particles on the biodegradability of the fibers was also evaluated. *In vitro* preliminary tests were performed to study the release of BSA from nanoparticle-laden fibers and to compare this with its release from free nanoparticles. Our results indicate that the distribution of particles inside the fibers was quite homogeneous and only a few of them were present on the surface. The presence of the particles in the fibers did not affect the thermal properties of the PCL polymer matrix, although it created voids that affected the degradation characteristics so the PCL fibers favored faster erosion compared to the plain fibers. Preliminary results indicate that the release from GNP-laden fibers occurred much more slowly compared to that in the free GNPs. © 2016 Wiley Periodicals, Inc. J. Appl. Polym. Sci. **2016**, *133*, 44233.

KEYWORDS: biodegradable; drug-delivery systems; fibers; proteins

Received 4 April 2016; accepted 24 July 2016
DOI: 10.1002/app.44233

INTRODUCTION

Peptides and proteins play a vital role in all biological processes and have received growing attention in recent years as drug candidates. Therefore, the ability to systemically deliver these compounds with adequate delivery systems is important.[1] However, some physicochemical and biological properties of protein and peptide drugs are different from those of conventional ones; these properties cause a number of limitations to their delivery.[2] Neither hydrophilic nor hydrophobic polymer systems are ideal for protein drug delivery. They each have advantages and disadvantages. Hydrophilic systems are compatible with protein drugs, but they are not suitable for sustained release because they absorb water and swell; this swelling causes protein molecules to rapidly diffuse out.[3] In contrast, hydrophobic systems are suitable for sustained drug release but are incompatible with water-soluble protein drugs. Their hydrophobicity may induce the unfolding of protein molecules, and therefore, protein drugs may lose their biological activity.[4] Our aim is to design and realize a polymeric system with combined hydrophilic–hydrophobic properties and based on poly(ε-caprolactone) (PCL) fibers loaded with gelatin nanoparticles (GNPs) containing bovine serum albumin (BSA) as a protein model. This combination would create a biodegradable system for protein delivery. PCL is a synthetic biodegradable aliphatic polyester that has attracted considerable research attention in recent years, especially for applications in the biomedical field. PCL can be spun into fibers and waved in textile structures. PCL fibers can be produced with diameters ranging from nanometers to millimeters. Because of their excellent biodegradability and biocompatibility characteristics, PCL fibers have been studied broadly for biomedical applications, such as bioresorbable constructs, drug-delivery systems, and tissue engineering scaffolds.[5–8]

The extrusion of PCL into monofilaments or multifilaments may be achieved by different fiber-formation mechanisms, including melt spinning, solution spinning, and electrospinning.[9–12] However, these extrusion procedures have limitations when biologically active agents have to be loaded into the fibers. When fibers are produced by melt spinning, high temperatures are required, and this may cause degradation of

pharmaceuticals.[13] In the case of wet spinning, only a small amount of active agent can be loaded because it dissolves in the coagulation fluid. During fiber formation, most drug molecules move from the polymer phase to the precipitation medium, and careful optimization of the coagulation and hardening stages is strictly necessary.[14] Electrospinning is another conventional method for producing fibers with a diameter on the order of nanometers. With this procedure, the type of solution and fluid properties, such as viscosity, surface tension, and vapor pressure, must be carefully adjusted to form a continuous and homogeneous-sized fiber. The presence of other components (active agents) in the polymer solution makes the previous parameters even more critical. Therefore, it is essential to disperse these components in the polymer solution as homogeneously as possible to ensure the formation of a uniform and continuous fiber.[15,16]

In this study, a simple and safe dry-spinning method was used to produce GNP-laden PCL fibers. Fiber formation was achieved by solvent evaporation at room temperature without a nonsolvent. At first, GNPs containing BSA were prepared by a two-step desolvation. Then, PCL fibers containing GNPs were produced by dry spinning and characterized by scanning electron microscopy (SEM), Fourier transform infrared (FTIR) microspectroscopy, and mechanical and thermal analysis. Preliminary biodegradation and *in vitro* release tests were also performed to test the ability of our system to load and subsequently release agents of a protein nature.

Our system is expected to offer several advantages. First, in dry spinning, the simple evaporation of the solvent at ambient temperature should preclude the need for nonsolvents and allow the loading of active agents without their alteration.

Second, two components of a different nature were combined: PCL fibers (hydrophobic) and GNPs (hydrophilic). This means that the system can offer the positive features of each of these.

A third element that makes the system interesting is that the loading of a drug into the particles, which are, in turn, inserted into fibers, slows down the diffusion process of the drug, and this yields a slower and more prolonged release.

Trapping GNPs into the PCL fibers yielded a combined hydrophilic–hydrophobic system with potential applications not only in the field of advanced drug release but also in the production of surgical sutures and bioactive scaffolds for tissue engineering. Such scaffolds, in addition to performing the usual support function for tissue regeneration, could be effective in the stimulation of several cell activities inside the construct, such as adhesion, proliferation, and differentiation, through the release of specific protein agents.

EXPERIMENTAL

Materials

Gelatin from bovine skin, glutaraldehyde, acetone, and BSA were purchased from Merck (Germany). PCL, with an average molecular weight of 80 kDa, and dichloromethane (DCM; 99.9% purity) were purchased from Sigma-Aldrich (Italy).

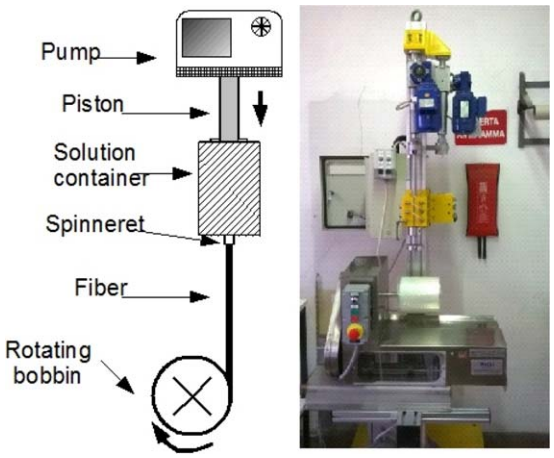

Figure 1. Schematic of the dry-spinning machine. [Color figure can be viewed at wileyonlinelibrary.com.]

Phosphate-buffered saline solution (PBS), with a pH of 7.4, was purchased from Sigma (Sigma no. D8537).

Preparation Methods

Preparation of the GNPs. GNPs were prepared through the modification of a two-step desolvation method proposed by Coester *et al.*[17] Briefly, 200 mg of gelatin was dissolved in 10 mL of distilled water under stirring at 40 ± 1 °C. Acetone (10 mL) was added to the gelatin solution to precipitate the high-molecular-weight gelatin fraction. The supernatant was discarded, and the high-molecular-weight gelatin fraction was redissolved through the addition of distilled water (10 mL) under stirring at 40 °C. BSA (2% w/w with respect to gelatin) was added; this was followed by the dropwise addition of acetone (30 mL) to form BSA-laden GNPs. At the end of the process, 100 μL of a 25% glutaraldehyde aqueous solution was added, and the solution was stirred at 40 ± 1 °C for 30 min. Finally, the solution was centrifuged at 11,790 relative centrifugal force (RCF) for 30 min. The obtained particles were purified by threefold centrifugation and redispersion in water, and then, they were freeze-dried to produce BSA-laden GNPs in the form of a white, freely flowing powder.

Fiber Production. A PCL solution (25% w/w) was prepared through the dissolution of the polymer in DCM at room temperature under stirring for about 24 h. The obtained solution was stored at room temperature for 12 h to eliminate the shear effect of stirring and to remove trapped fine air bubbles. Microfibers were produced by a dry-spinning process. We forced the polymer solution through a needle with a diameter of 0.65 mm. As the polymer solution exited the needle (spinning speed = 7 cm/s), a fiber was formed because of solvent evaporation in the air gap (10 cm) between the needle and the collecting bobbin (Figure 1). The *draw ratio*, defined as the ratio of the take-up velocity to the extrusion velocity, was 7.

The same procedure was used to produce the GNP-laden PCL fibers. For preparation of the solution, first, the GNPs were dispersed in DCM by sonication (Hielscher ultrasonic processor UP 400 S). The suspension was sonicated three times (each time for 2 min) at full power (400 W) and at a frequency of

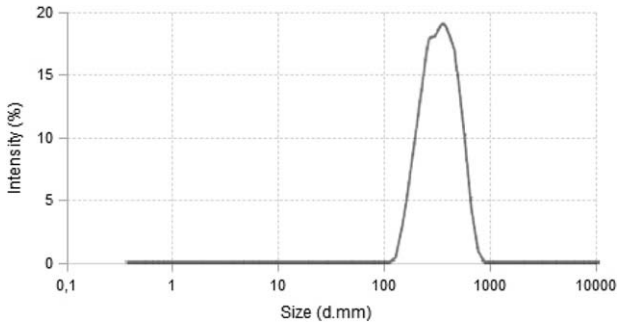

Figure 2. Size distribution of GNPs produced by a two-step desolvation method.

24 kHz by a 3-mm sonotrode. Then, PCL was added, and the solution was left at room temperature for about 24 h under mechanical stirring to form a homogeneous dispersion. The concentration of the GNPs was 2% w/w with respect to PCL.

Characterization

Morphological Properties. The morphology and size distribution of the GNPs were investigated with SEM (KYKY EM-3200) and dynamic light scattering (Malvern Zen3600 Zetasizer). The particles were coated with a thin layer of gold before analysis.

The morphology of the fibers was also investigated by SEM (JEOL JSM-5600 LV). The fibers were first freeze-fractured in liquid nitrogen and then coated with a thin layer of gold before analysis.

Drug Loading. The amount of BSA present in the nanoparticles was determined by an indirect method. During nanoparticle preparation, after the final solution centrifugation, the supernatant was removed and analyzed by high-performance liquid chromatography (HPLC; PerkinElmer, series 200, equipped with a ProSphere HP C4 300 Å, 5 μm, length = 250 mm and *i.d.* = 4.5 mm) to determine the amount of free BSA. The first mobile phase was a mixture of water and trifluoroacetic acid (0.08% v/v), whereas the second mobile phase was a mixture of acetonitrile–water (95/5 v/v) and trifluoroacetic acid (0.065% v/v). A flow rate of 1 mL/min was used, and BSA was detected at a λ of 280 nm.

The BSA entrapment efficiency of the GNPs was calculated as follows:

$$\text{Entrapment efficiency} = [(Q_{\text{Total}} - Q_{\text{Free}})/Q_{\text{Free}}] \times 100 \quad (1)$$

where Q_{Total} and Q_{Free} are the total BSA used and the amount of free BSA, respectively.

Release Testing. The weighted samples of the BSA-laden GNPs (5 mg) were combined with 10 mL of PBS (pH 7.4). The samples were kept at 37 °C under stirring. At predefined time intervals, the samples were centrifuged at 3225 RCF for 5 min, and 2 mL of the resulting supernatants was removed, replaced with fresh PBS, and analyzed with HPLC at a λ of 280 nm. To measure the release of BSA from the GNPs loaded into the fibers, weighed samples of fibers (250 mg) were combined with 10 mL of PBS and kept at 37 °C under stirring at 155 OPM. At defined time intervals, 2 mL of each eluate was removed, replaced with 2 mL of fresh PBS, and analyzed by HPLC at a λ of 280 nm.

Mechanical Properties. The tensile strength and Young's modulus values of both the plain and GNP-laden PCL fibers were determined with an Instron 5542 dynamometer used in tensile mode. The load cell had a maximum capacity of 5 N. The selected gauge length and crosshead speed were 10 mm and 25 mm/min, respectively. Randomly selected fibers were tested. For each type of fiber, the results of six replicates were averaged and are reported. An analysis of variance test was used to calculate the significance level ($p < 0.05$).

Thermal Properties. The thermal behavior of the plain and GNP-laden PCL fibers was investigated with differential scanning calorimetry (DSC; DSC7, PerkinElmer). The samples were sealed in aluminum pans and heated from 20 to 120 °C at a rate of 10 °C/min. For each type of fiber, the results of five replicates were averaged and are reported. An analysis of variance test was used to calculate the significance level ($p < 0.05$).

FTIR Microspectroscopy [Microattenuated Total Reflectance (μATR)–FTIR]. Spectral images were acquired in both transmission and μATR modes with a Spotlight 300 IR imaging system (PerkinElmer). The spectral resolution was 4 cm^{-1}. The spatial resolution was 6.25 μm in transmission mode and 100 × 100 μm in μATR mode. Background scans were obtained from a region with no sample. IR images were acquired with a liquid-nitrogen-cooled mercury cadmium telluride line detector composed of 16 pixel elements. Each absorbance spectrum composing the IR images and resulting from 16 scans was recorded for each pixel in μATR mode with the Spotlight software. We collected the spectra by touching the attenuated total reflectance objective on the sample and collecting the spectrum generated from the surface layer. The Spotlight software used for the acquisition was also used to preprocess the spectra. IR spectral images were produced with the absorbance in a given frequency range of 4000–720 cm^{-1}.

Degradability. Samples of both the loaded and plain fibers were combined with PBS and incubated at 37 °C with shaking for a period of 4 months. At the end of the incubation period, SEM analysis was carried out to evaluate possible morphological changes in the fibers. The fiber samples were collected and vacuum-dried for 1 day at 30 °C. The dried samples were weighed with an electronic balance, and the degradation degree was calculated as follows:

$$\text{Degradation degree} = [1 - (W_t/W_t)] \times 100 \quad (2)$$

where W_t is the dry weight after incubation time t and W_i is the initial dry weight.

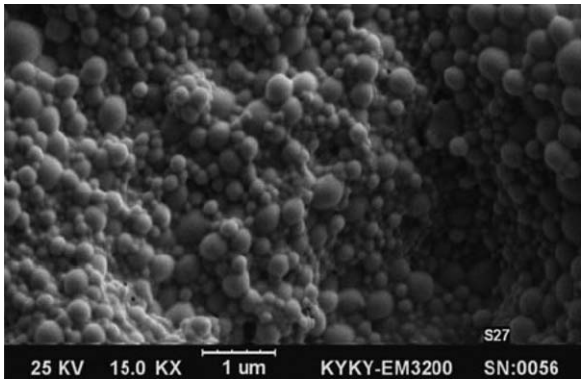

Figure 3. SEM image of GNPs.

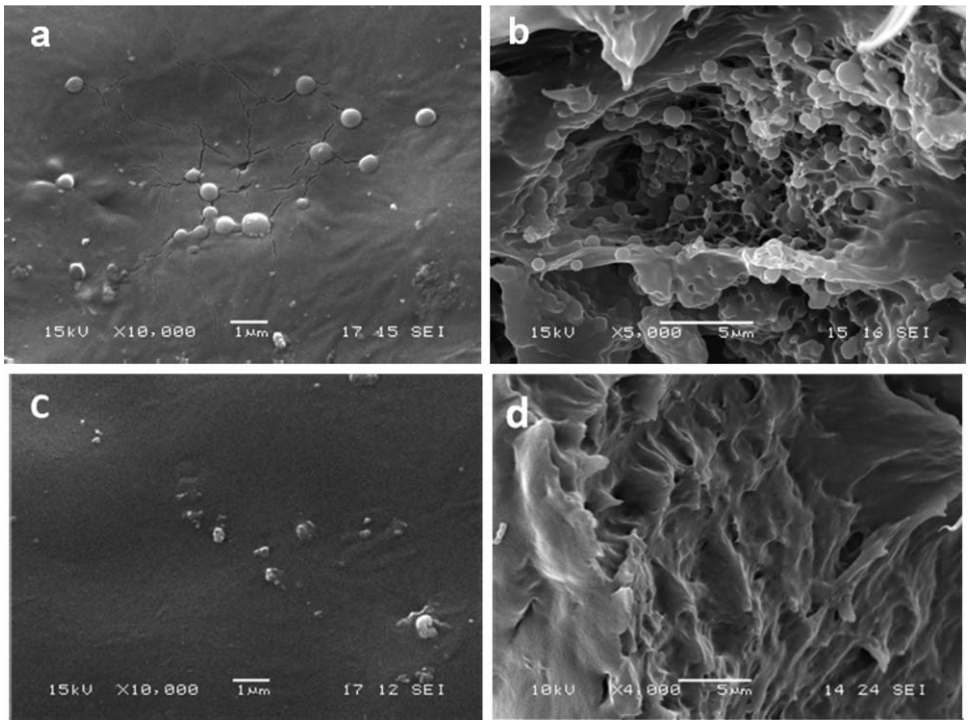

Figure 4. SEM images of the (a) surface and (b) cross-section of the GNP-laden fibers and the (c) surface and (d) cross-section of the plain fibers.

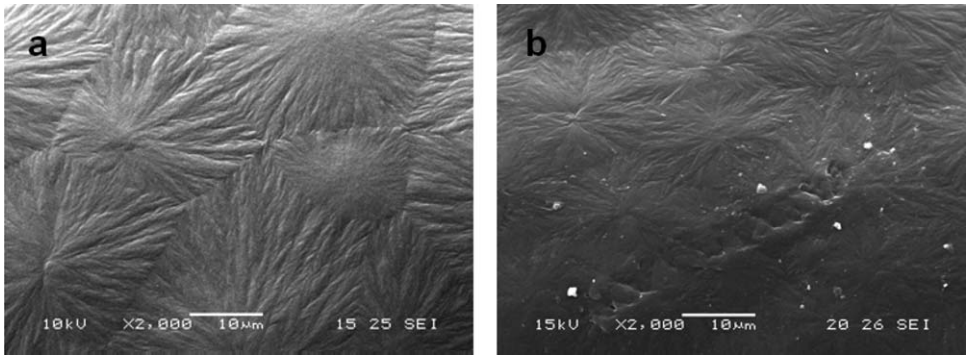

Figure 5. SEM images of the fiber surfaces: (a) PCL and (b) GNP-laden PCL fibers.

RESULTS AND DISCUSSION

Morphological Properties

The size distribution of the produced particles is shown in Figure 2, whereas the SEM image of the GNPs is shown in Figure 3.

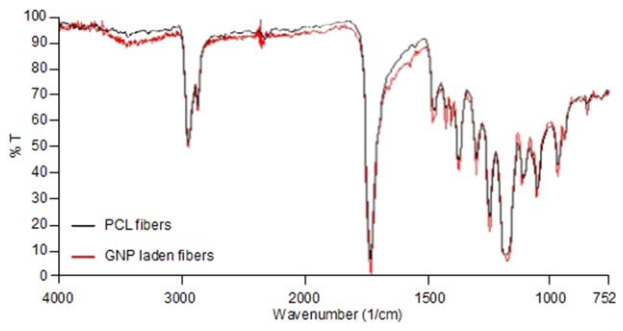

Figure 6. Spectra of the plain and GNP-laden fibers recoded in the μATR mode. [Color figure can be viewed at wileyonlinelibrary.com.]

For the produced particles, an average diameter of 290 nm was found, and a polydispersity index of 0.26 was calculated. This parameter describes the degree of nonuniformity of a distribution.[18] The value found was in the 0.0–0.4 range and indicated that the system was moderately polydispersed. The SEM images indicated that the particles were smooth and spherical and lacked hairline cracks and heterogeneities on their surface.

PCL fibers containing GNPs were successfully produced. The diameters of both the plain and GNP-laden PCL fibers were in the range 100–200 μm, and the presence of GNPs did not dramatically affect the fiber diameter. The surface and cross section of a the GNP-laden PCL fibers are shown in Figure 4(a,b). The cross section of the PCL fibers is shown in Figure 4(c). Most particles were distributed inside the fiber, and only a few were found on the surface. This indicated a negligible segregation effect during fiber production. Also, the fibers loaded with the particles had voids in their interior.

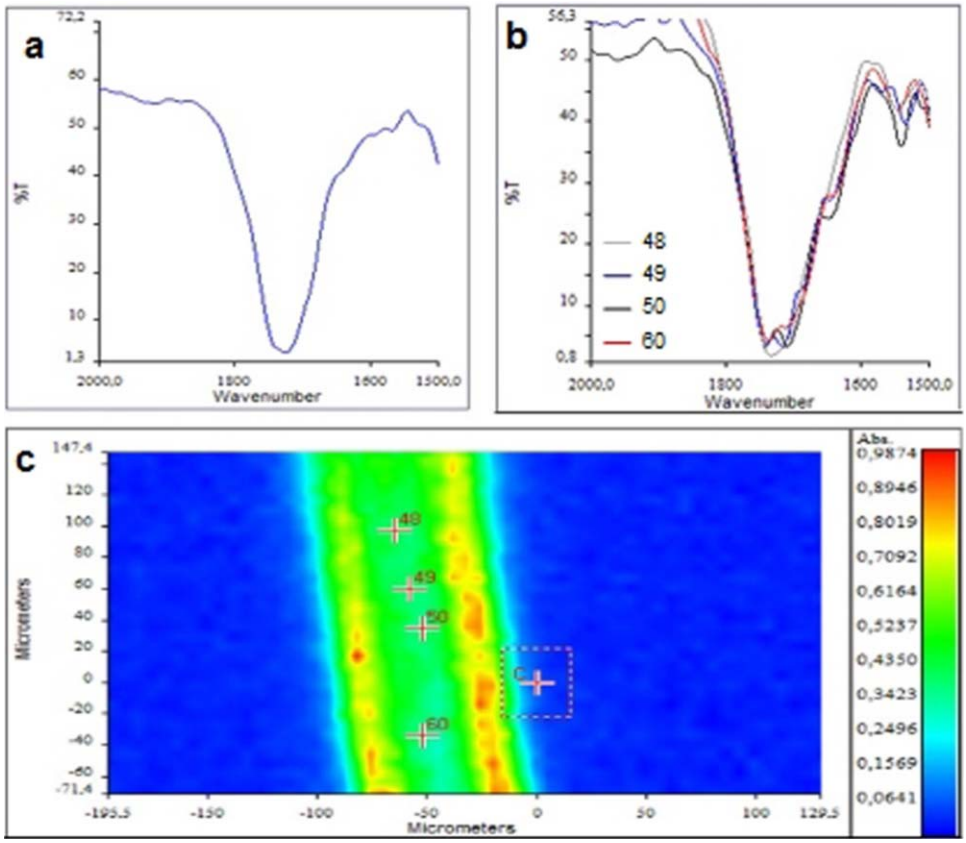

Figure 7. (a) Spectrum of the PCL fibers, (b) spectrum of the GNP-laden PCL fibers acquired at different positions (numbered 48, 49, 50, and 60), and (c) chemical maps of the GNP-laden PCL fibers. [Color figure can be viewed at wileyonlinelibrary.com.]

From these observations, we inferred that the method used for the production of the fibers yielded a quite homogeneous distribution of the particles inside them. The formation of the fibers after solvent evaporation occurred rapidly, and the particles did not have sufficient time to migrate to the surface and remain locked within the fiber because of their small size and the density of the polymer solution they were dispersed in. The particles were unlikely to be lost during the production of the fibers; therefore, with the particles as a carrier, it appeared possible to load a substantial amount of the drug of interest into the fibers.

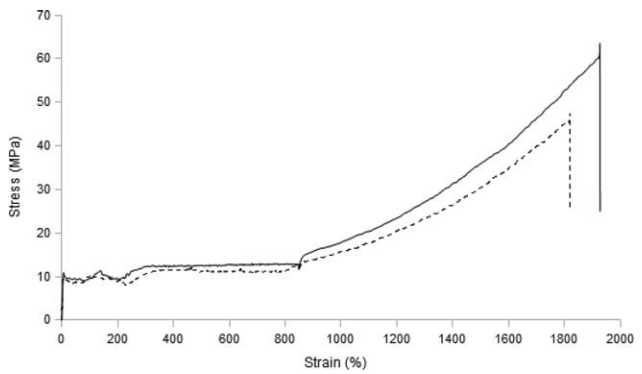

Figure 8. Tensile properties of the (—) PCL and (- - -) GNP-laden PCL fibers.

Figure 5 shows images of the surface of both the plain [Figure 5(a)] and GNP-laden [Figure 5(b)] PCL fibers. Both showed the presence of crystal structures, and no relevant differences were observed.

μATR–FTIR Microspectroscopy

μATR–FTIR microspectroscopy was used to evaluate the presence of GNPs on the surface of the fibers. Figure 6 shows the spectra of both the plain and GNP-laden PCL fibers acquired in μATR mode. No evident difference was observed between the two spectra. As shown in Figure 4, the amount of particles on the surface of fibers was too low to be revealed by this analysis.the spectra recoded in transmission mode are shown in Figure 7.

Figure 7(a) shows the spectrum of a plain PCL fiber, whereas Figure 7(b) shows the spectra acquired at different positions [indicated by marks in Figure 7(c)] from an image of the GNP-laden fibers. Common protein bands were present at approximately 1650 cm^{-1} (amide I) and 1540 cm^{-1} (amide II); these corresponded to the stretching vibrations of the C═O bond, coupled with the bending of the N─H bond and the stretching of the C─N bond, respectively. These protein bands indicated the presence of the particles inside the fibers and confirmed the results obtained by SEM analysis.

Tensile Properties

Knowing the mechanical properties of materials is important for evaluating their suitability for tissue engineering scaffolds.[19] The tensile properties of both the plain and GNP-laden PCL

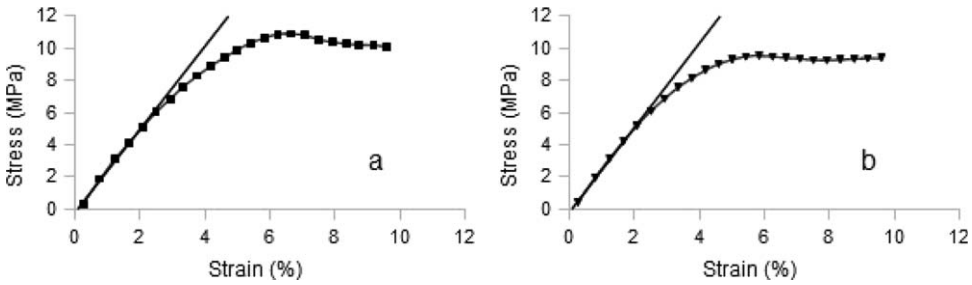

Figure 9. Stress–strain graph of the (a) plain and (b) GNP-laden PCL fibers. The elastic modulus was calculated as the slope of the initial portion of the curve.

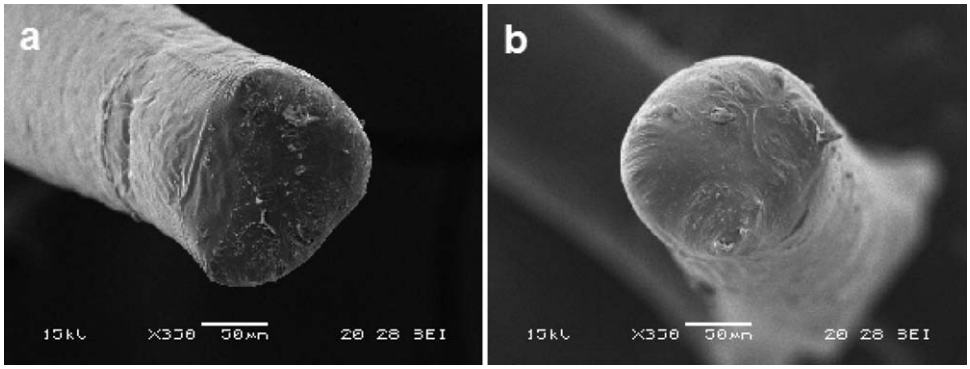

Figure 10. Cross-sections of the (a) plain and (b) GNP-laden PCL fibers.

fibers were evaluated at room temperature. The stress–strain curves for the plain and GNP-laden fibers are reported in Figure 8. The usual trend for an elastoplastic polymer was observed.

After a short initial portion (up to a strain of 7–8%) in which the stress increased with strain, the value of the stress remained almost constant up to a value of strain equal to 900%. Beyond this point, the alignment of the chains of the amorphous portion was complete, and the stress increased again up to a breaking point. The value of the elastic modulus was calculated for both types of fibers as the slope of the initial portion of the stress–strain curve [Figure 9(a,b)]. SEM images of the fiber cross sections were used to calculate the modulus values (Figure 10).

For the plain fibers, we found a modulus equal to 294 ± 22 MPa, whereas for the loaded fibers, we found a value of 260 ± 15 MPa. The two values were different from a statistical point of view ($p < 0.05$), and this difference was attributed to the presence of particles.

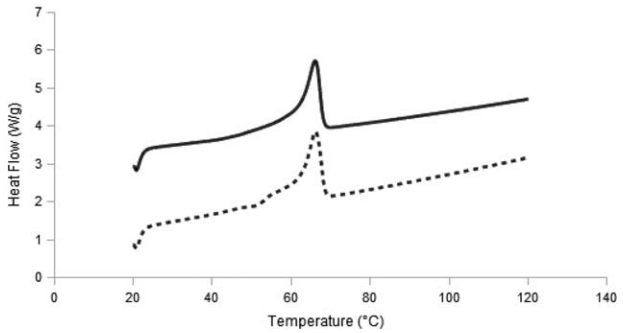

Figure 11. DSC thermograms of the (—) plain and (- - -) GNP-laden PCL fibers.

The GNP-laden PCL fibers exhibited a tensile strength of 45 ± 2 MPa; this was lower than that found for plain fibers, for which a value of 64.4 ± 3.1 MPa was determined ($p < 0.05$). Similar results were found for the elongation at break: a value of $1940 \pm 90\%$ was found for the plain fibers, and a value of $1810 \pm 80\%$ was found for the loaded fibers ($p < 0.05$). This suggested that the particles loaded into the fibers acted as defects without, however, substantially modifying the structure of the PCL polymeric matrix.

Thermal Properties

The effect of the GNPs on the thermal characteristics of the dry-spun PCL fibers was investigated by DSC. DSC thermograms of the plain and GNP-laden PCL fibers are shown in Figure 11. There were no significant differences ($p > 0.05$) between the two types of fibers with regard to both the melting point and melting enthalpy (Table I). Therefore, the same was concluded for the degree of crystallinity, which we calculated by dividing the measured melting enthalpy by 136 J/g, which was the theoretical melting enthalpy for 100% crystalline PCL.[19] These results indicate that the addition of the used amount of

Table I. Thermal Properties of the Plain and GNP-Laden PCL Fibers

Sample	Melting point (°C)	Melting enthalpy (J/g)	Crystallinity (%)
Plain fibers	66.0 ± 0.2	70.8 ± 1.8	52.1 ± 1.3
GNP-laden fibers	66.3 ± 0.1	71.6 ± 3.0	52.6 ± 2.2

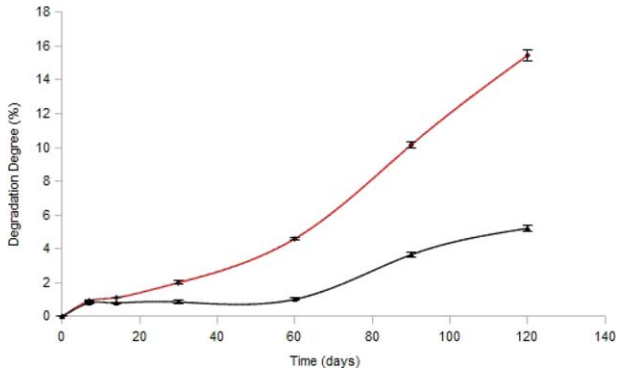

Figure 12. Degradation of the plain PCL fibers (black line) and GNP-laden PCL fibers (red line) as a function of time. [Color figure can be viewed at wileyonlinelibrary.com.]

particles did not alter either the nature of crystals or the degree of crystallinity of the material.

Degradation of the PCL and GNP-Laden Fibers

It is widely accepted that the hydrolytic degradation of poly(α-hydroxy esters) can proceed via surface or bulk degradation pathways. Surface degradation and erosion involve the hydrolytic cleavage of the polymer backbone only at the surface. This occurs when the rate of hydrolytic chain scission is faster than the rate of water intrusion into the polymer bulk. Bulk degradation occurs when water is able to enter the whole polymer bulk; it results in hydrolysis throughout the entire polymer matrix.[20] The degradation of the plain and GNP-laden fibers was investigated during a 4-month period. The results of the *in vitro* analysis showed a higher mass loss for the loaded fibers than for the plain fibers (Figure 12).

The degradation of the plain fibers seemed to occur through a surface pathway, which resulted in a slow erosion. The hypothesis was that in the case of the GNP-laden fibers, voids were introduced through the hydrophilic GNP phase [Figure 4(b)]. Thus, a larger surface area was provided for water attack. Therefore, because of enhanced hydrolysis, these fibers eroded faster than the plain fibers.

In Figure 13, both loaded and plain fibers before and after 4 months of degradation are shown. The plain fibers [Figure 13(a,b)] did not show significant signs of degradation, whereas the morphology and integrity of the GNP-laden fibers [Figure 13(c,d)] results were significantly altered.

In Vitro Release Test

The total amount of BSA released by the GNPs was about 87% of the initial amount used for sample loading. The release profile of BSA from the GNPs was obtained by HPLC. A standard curve was obtained with five different concentrations of BSA. Figure 14(a) illustrates the BSA release profile from the GNPs at 37 °C during 7 days of incubation. It was possible to observe an initial phase of rapid release [burst release phase; Figure 14(b)] followed by a slow release, which lasted several days. More than 70% of BSA contained in the particles was released within about 3 days. The burst release phase may have been due to the BSA molecules embedded in the surface or near the external surface of the GNPs. A reduction in the release rate may have been due to the reduced concentration of BSA in the gelatin matrix.

The mechanism of protein release from the GNPs may have involve the following aspects: (1) water permeation through the hydrogel matrix and absorption by the GNPs, (2) GNP swelling, and (3) diffusion of BSA molecules through the swollen GNPs. The release of BSA from the GNPs entrapped in the PCL fibers

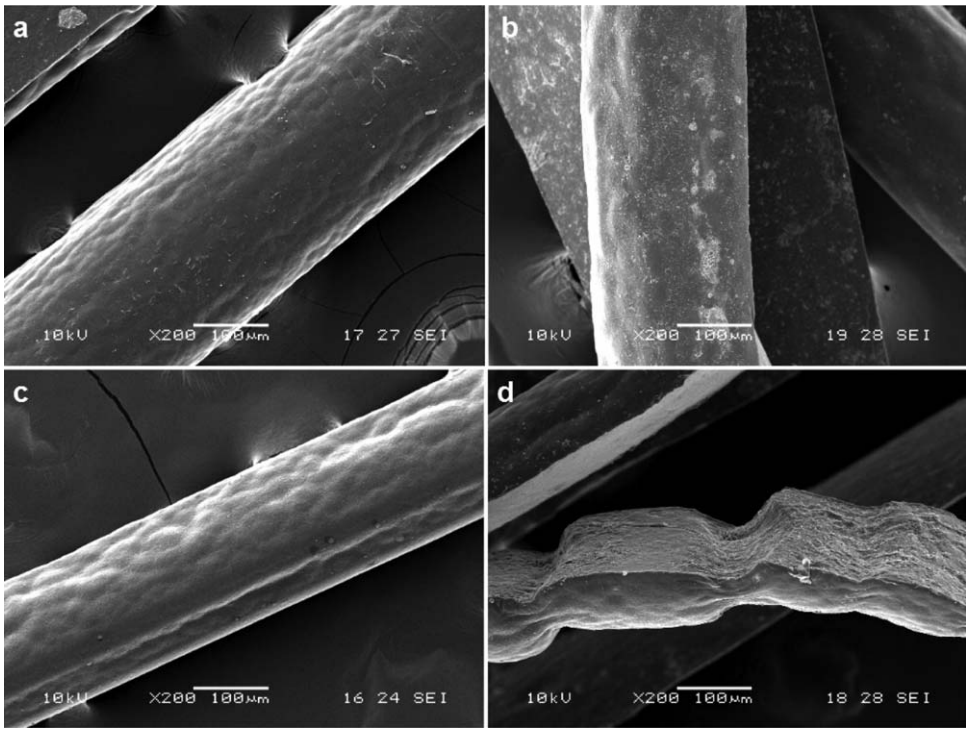

Figure 13. SEM images of the fiber surfaces (a,c) before and (b,d) after 4 months of incubation: (a,b) plain and (c,d) GNP-laden PCL fibers.

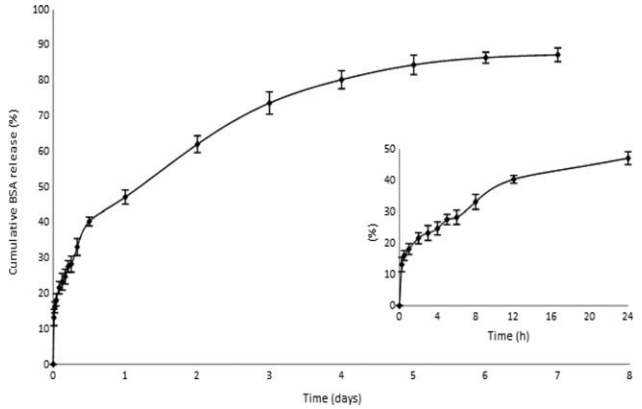

Figure 14. Cumulative percentage of BSA released from GNPs as a function of time after 7 days of incubation. The insert shows the details for the first 24 h.

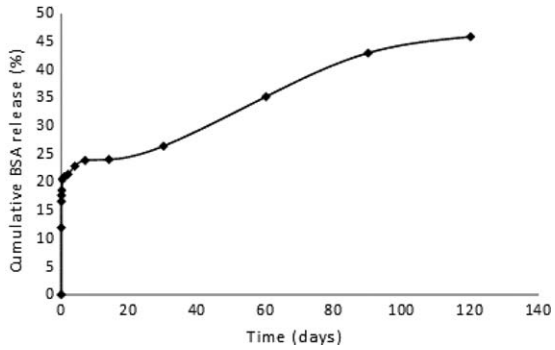

Figure 15. Cumulative percentage of BSA released from GNPs entrapped in the PCL fibers as a function of time.

was investigated during a 4-month period (Figure 15). The release trend was similar to that of free nanoparticles, but the release occurred much more slowly. In fact, after about 3 days, the percentage release was around 20%.

A schematic of the system is shown in Figure 16(a,b). The mechanism of release might have involved the following aspects. In the first phase, before the beginning of the degradation of both fibers and particles, the release of BSA occurred only by diffusion. By absorbing water, BSA first diffused out of the particles [Figure 16(c)] and then passed through the fiber [Figure 16(d)]. This was a two-step diffusion process with apparently slow kinetics. However, the BSA release was affected by the surface-to-volume ratio of the particles and by the thickness of the fiber. The initial burst phase was connected with the BSA within the particles on the surface or near the inner wall of the fibers [Figure 16(d)]. Subsequently, when fiber biodegradation was started, a larger surface area was provided for water attack, and there was more space for water to penetrate and head toward the GNPs located in the interior parts of the fiber. So, water provided more BSA passages through the fiber and more BSA release [Figure 16(e)]. So at this step, the kinetics of drug release depended on both diffusion and

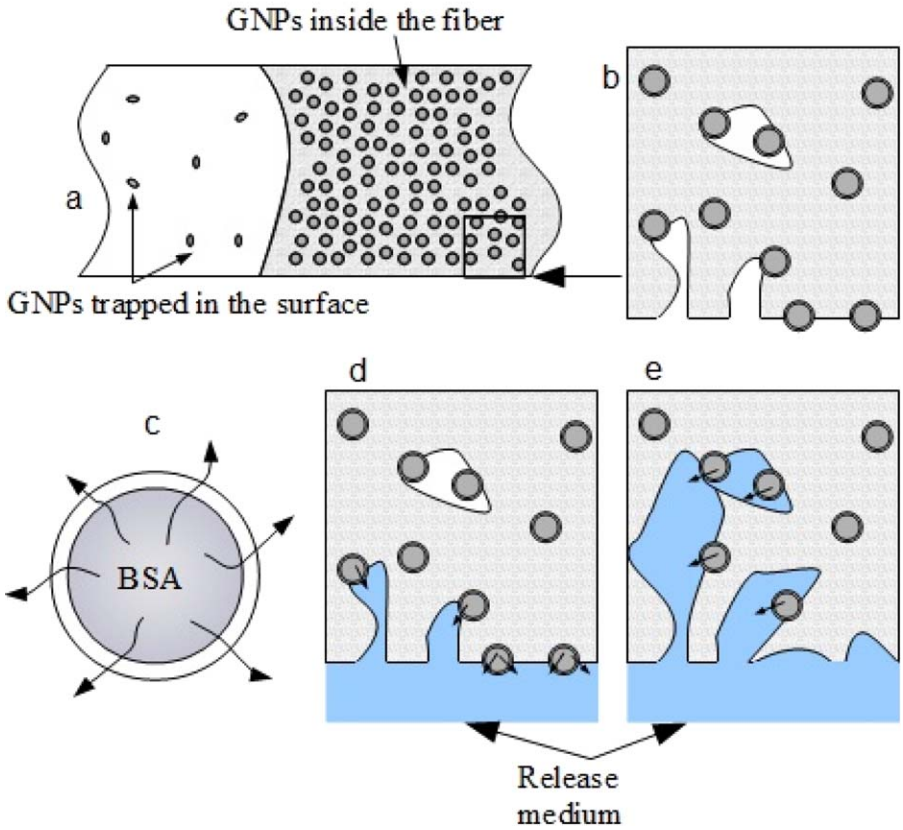

Figure 16. (a,b) Schematic representation of the system, (c) diffusion of BSA through GNPs, (d) release of BSA from GNPs located in the surface and near inner wall of the fibers, and (e) release of BSA from GNPs located in the interior part of the fibers due to biodegradation. [Color figure can be viewed at wileyonlinelibrary.com.]

fiber degradation. As shown in Figure 12, GNP-laden fibers started to degrade sharply after about 40 days. The incisive increase in BSA release around 40–80 days could have been related to the onset of fiber biodegradation (Figure 15).

CONCLUSIONS

A simple dry-spinning method was used to produce PCL fibers containing BSA-laden GNPs. The nanoparticles, produced by a two-step desolvation method, were homogeneously distributed inside the fibers, and their addition did not substantially change the properties of the polymeric PCL matrix. This system with combined hydrophilic–hydrophobic properties was designed to create a compatible matrix for drugs of a protein nature and their release directly to the desired target. Several features make this system suitable for the creation of advanced drug-delivery systems, biodegradable sutures, and bioactive scaffolds for tissue engineering. First, the release of the BSA could be made complete by the biodegradation of both fiber and particles. Second, it is likely that time-release profiles could be modulated through an appropriate combination of physical, chemical, and technological parameters. Third, this system offers the possibility of simultaneously issuing various drugs loaded into different particles, with each drug being characterized by its own release profile.

Moreover, because of the mild operative conditions required, the dry-spinning method could prove to be suitable for creating fiber-particle composite systems in which components of any sensitive nature are preserved.

REFERENCES

1. Al-Tahami, K.; Singh, J. *Rec. Pat. Drug Delivery Formul.* **2007**, *1*, 65.
2. Shaji, J.; Patole, V. *Indian J. Pharm. Sci.* **2008**, *70*, 269.
3. Li, J. K.; Wang, N.; Wu, X. S. *J. Microencapsul.* **1998**, *15*, 163.
4. Zamani, M.; Prabhakaran, M. P.; Ramakrishna1, S. *Int. J. Nanomed.* **2013**, *8*, 2997.
5. Williamson, M. R.; Coombes, A. G. A. *Biomaterials* **2004**, *25*, 459.
6. Chang, H. I.; Lau, Y. C.; Yan, C.; Coombes, A. G. A. *J. Biomed. Mater. Res. A* **2008**, *84*, 230.
7. Puppi, D.; Piras, A. M.; Chiellini, F.; Chiellini, E.; Martins, A.; Leonor, I. B.; Neves, N.; Reis, R. *J. Tissue Eng. Regen Med.* **2011**, *5*, 253.
8. Puppi, D.; Dinucci, D.; Bartoli, C.; Mota, C.; Migone, C.; Dini, F.; Barsotti, G.; Carlucci, F.; Chiellini, F. *J. Bioact. Compat. Polym.* **2011**, *26*, 478.
9. Charuchinda, A.; Molloy, R.; Siripitayananon, J.; Molloy, N.; Sriyai, A. M. *Polym. Int.* **2003**, *52*, 1175.
10. Azimi, B.; Nourpanah, P.; Rabiee, M.; Arbab, S. *J. Eng. Fiber Fabr.* **2014**, *9*, 74.
11. Puppi, D.; Detta, N.; Piras, A. M.; Chiellini, F.; Clarke, D. A.; Reilly, G. C.; Chiellini, E. *Macromol. Biosci.* **2010**, *10*, 887.
12. Azimi, B.; Nourpanah, P.; Rabiee, M.; Cascone, M. G.; Baldassare, A.; Lazzeri, L. *J. Appl. Polym. Sci.* **2015**, *132*, DOI: 10.1002/app.42113.
13. Nguyen, K. T.; Su, S. H.; Sheng, A.; Wawro, D.; Schwade, N. D.; Brouse, C. F.; Greilich, P. E.; Tang, L.; Eberhart, R. C. *Biomaterials* **2003**, *24*, 5191.
14. Williamson, M. R.; Chang, H.; Coombes, A. G. A. *Biomaterials* **2004**, *25*, 5053.
15. Shin, S. H.; Purevdorj, O.; Castano, O.; Planell, J. A.; Kim, H. W. *J. Tissue Eng. Regen. Med.* **2012**, *3*, 1.
16. Kim, H. W.; Lee, H. H.; Knowles, J. C. *J. Biomed. Mater. Res.* **2006**, *79*, 643.
17. Coester, C. J.; Langer, K.; Briesen, H. V.; Kreuter, J. J. *Microencapsul.* **2000**, *17*, 187.
18. Nobbmann, U. Polydispersity—What Does It Mean for DLS and Chromatography? http://www.materials-talks.com/blog/2014/10/23/polydispersity-what-does-it-mean-for-dls-and-chromatography/(accessed October 23, **2014**).
19. Gaharwar, A. K.; Mukundan, S.; Karaca, E.; Dolatshahi-Pirouz, A.; Patel, A.; Rangarajan, K.; Mihaila, S. M.; Iviglia, G.; Zhang, H.; Khademhosseini, A. *Tissue Eng. A* **2014**, *20*, 2088.
20. Lam, C. X.; Hutmacher, D. W.; Schantz, J. T.; Woodruff, M. A.; Teoh, S. H. *J. Biomed. Mater. Res. A* **2008**, *90*, 906.